Tandem Electron Beam Welding (Report-II)†

Yoshiaki ARATA*, Eiji NABEGATA** and Nobuya IWAMOTO*

Abstract

In case of the deep penetration welding by using the conventional single electron beam welding method, it was seen that the occurrence of internal defects is closely related with the configuration of the weld root with small radius of curvature formed by a narrow diameter beam in high power density. In this weld root, the molten metal is hardly deposited and its cooling-rate is very fast compared with the case of shallow and wide sound weld bead produced by a wide diameter beam in low power density.

By the use of the TANDEM ELECTRON BEAM WELDING method, the occurrence of internal defects can be sucessfully prevented and occurence of internal defects can be sucessfully prevented and sound bead is obtained even at the deep penetration condition where the internal defects appear by using the single electron beam welding. In this system, a wide diameter beam of EB-2 in low power density fully penetrates over the depth where the defects are caused by a high power density beam of EB-1. A new and large radius of weld root is produced by EB-2 and its weld root is easily deposited with the molten metal in low cooling-rate.

1. Introduction

As is well known, electron beam welding method has a superiority in obtaining a deep penetration weld by the low input welding power compared with the arc welding method since the beam is utilized in very high power density. However such high power density usually brings about a serious problem of the occurrence of internal defects such as the Spiking, Cold - shut and Porosity which would weaken the mechanical strength of the weld part.

Some investigations[1),2),3)] concernning with the appearances of the internal defects have been reported. In recent conventional single electron beam (SEB) welding, these internal defects are avoided by oscillating or diverging the beam, but by which the welding speed[4)] is decreased and the weld bead becomes shallow, so the superiority of the electron beam welding is spoiled.

The aim of this work is to clarify the fundamental parameters governing the formation phenomena of the internal defects, and to prove the possibility of preventing the internal defects even at the deep penetration condition by the use of the TANDEM ELECTRON BEAM WELDING (TEB-Welding)[4),5)] method.

2. Experimental Apparatus and Procedure

Schematic diagram of the TEB-WELDER is shown in **Fig. 1**. Two electron beams are produced by Gun-1 & Gun-2 which are settled compactly, and EB-1 is perpendicularly supplied on the surface of a specimen, while EB-2 is controlled to be impinged on the proper position of the specimen surface using the beam deflector.

EB-1 is used as a heat source to melt the specimen with deep penetration, and EB-2 is used to enlarge the beam hole and to control the configuration of weld root. Each beam power (W_b) can be selected independently and its maximum beam power is 6 KW respectively. In this work, the beam diameter (d_b) is determined from its spatial distribution using the Faraday-cup as shown in **Fig. 2**, and by which the distribution signal of the electron beam current is typically shown in **Photo. 1**. Namely as shown in **Fig. 3**, the beam radius (r_b) is regarded as a distance where the density of beam currents falls to 1/e of its axial value. Using this beam radius, the power density (w_b) is estimated; $w_b=w_b/(\pi r^2{}_b)$. Welding speed of this apparatus is in the range of 12cm - 11.2m/min.

Besides, to evaluate the ability of the weld penetration, the effective penetroparameter[5)] $\tilde{p}_p$ is introduced as shown in **Fig. 4**; $\tilde{p}_p=\bar{h}_p/\bar{d}_B$ here $\bar{h}_p$ and $\bar{d}_B$ show the

† Received on 9th October, 1978
* Professor, Director
** Research Associate

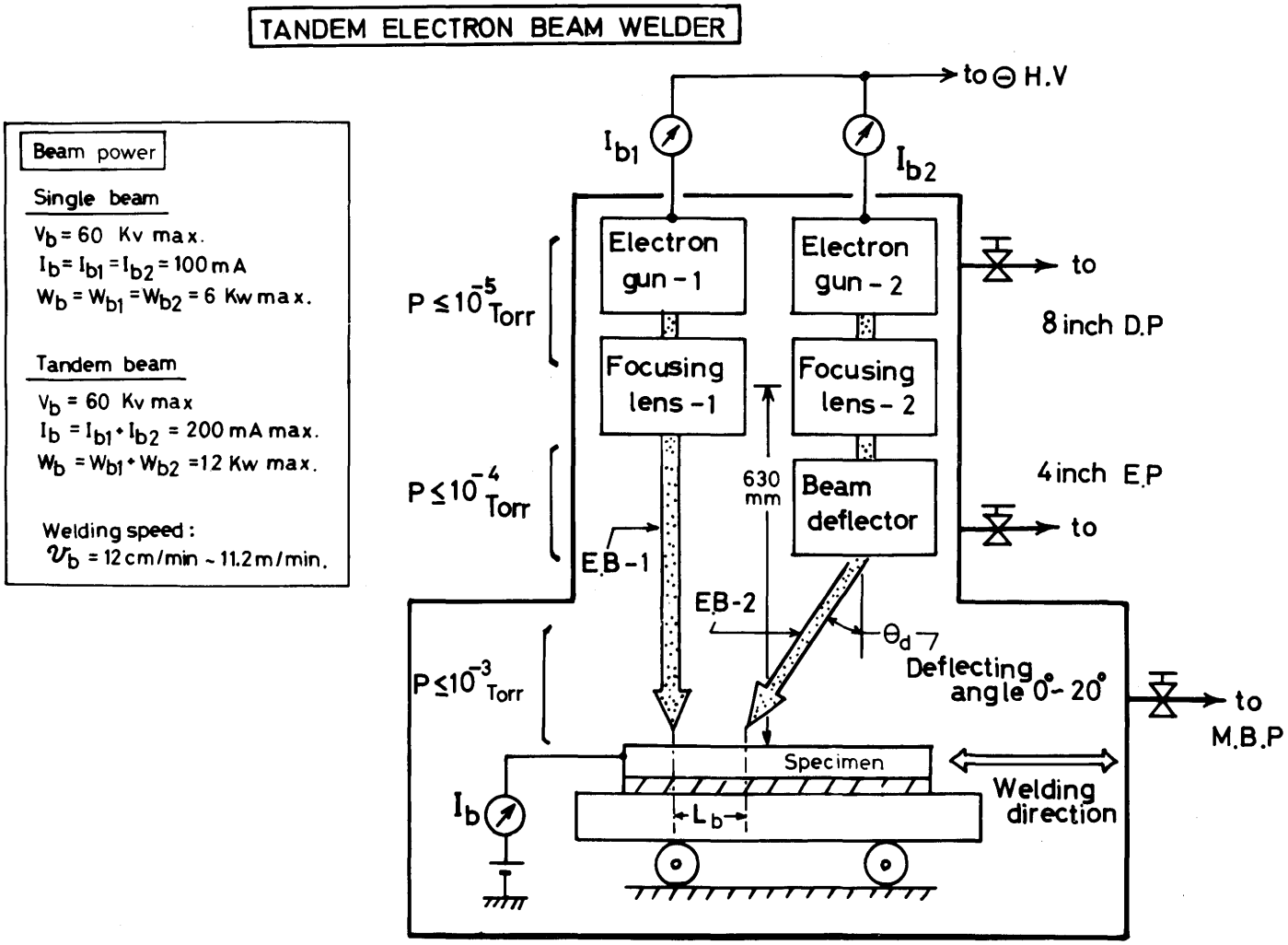

Fig. 1 Schematic diagram of TEB-WELDER.

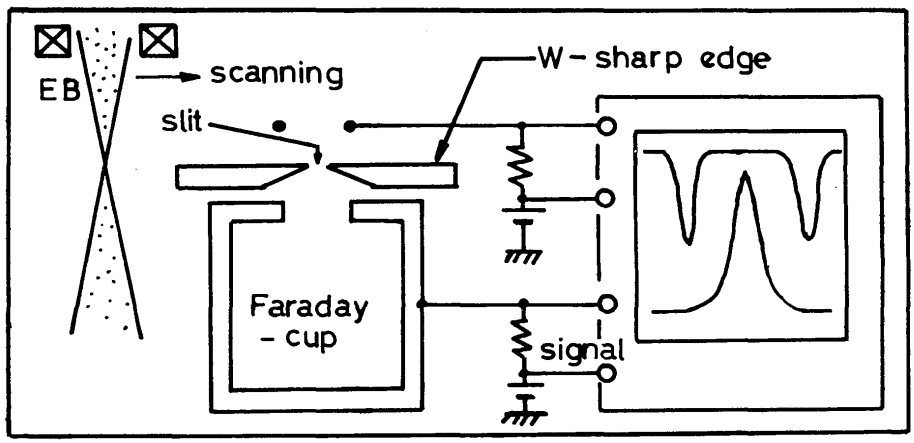

Fig. 2 Method of measuring beam diameter by using Farady-cup.

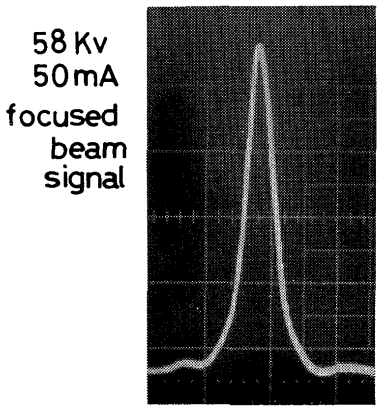

Photo. 1 Typical signal of electron beam current by using Faraday-cup.

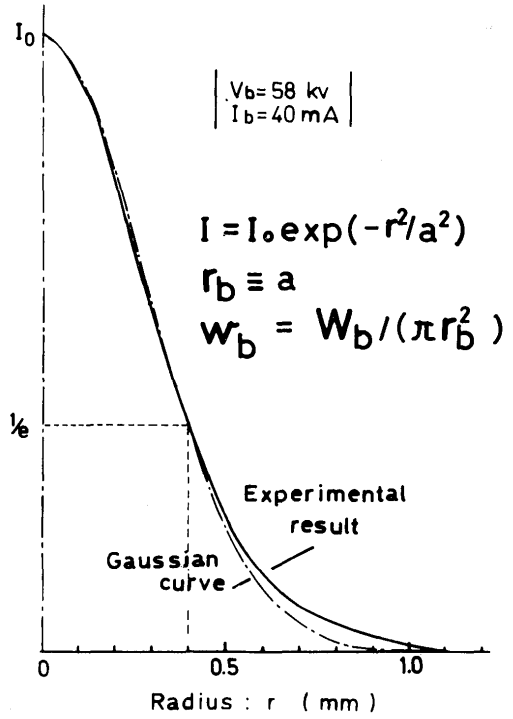

Fig. 3 Distribution of beam current density through Abel's conversion.

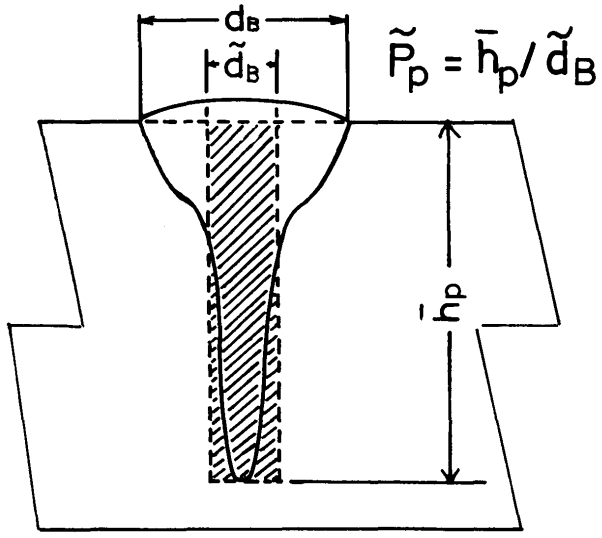

Fig. 4 Evaluation of penetration weld bead by Effective penetro-parameter $\tilde{P}p$.

average penetration depth and average bead width respectively. Specimen used are two kinds of the Al-Mg alloy and Al-Mg-Zn alloy metals, their chemical compositions are shown in **Table 1**, and the size of specimen is 300mm in length, 18mm in width, and 60mm in thickness. All experiments were carried out in bead-on-plate welding.

Chemical composition of specimen used

element / material	Al	Cu	Si	Fe	Mn	Mg	Zn	Cr	Ti
Al 5083 (50mmt)	Bal	0.02	0.09	0.24	0.67	4.6	0.01	0.13	0.03
Al 7075 (60mmt)	Bal	2.3	0.13	0.35	0.10	3.6	7.0	0.19	0.04

wt(%)

Table 1 Chemical compositions of specimens used.

3. Single Electron Beam Welding

3.1 Various internal defects

In the conventional single electron beam welding (SEB-Welding) method, typical three kinds of the internal defects are shown in **Photo. 2**. One is Spiking which is a kind of the uneven-penetration. The second is Root-Porosity or R-Prosity which usually appears in the tips of the weld root with Spiking. The third is "Cold-shut"[5),6)] which is the incomplete coalecence line along the equi-solidification front in the weld bead.

3.2 Characteristics of Internal Defects

In **Fig. 5**, number of such internal defects per unit length along the welding direction is shown versus the effective penetroparameter $\tilde{p}_p$. In this figure, the square and circle marks indicate the case of Cold-shut and R-Porosity respectively. These plots are obtained by changing the welding speed, beam power and power dinsity in wide range. Clearly we find no-defects in case of the shallow and wide beads of $\tilde{p}_p \leqq 5$.

The relation between the beam power density and the number of defects are shown in **Fig. 6** and **7**. In Fig. 6, the beam power density is selected by changing the beam diameter on the spacimen surface at the constant beam power. Using the high power density beam in small diameter, the sharp needle like weld root is formed with the deep penetration condition containing the defects. While, using the low power density beam with wide diameter, the round and sound weld root in shallow penetration is produced without defects as is illustrated in the figure. Typical cross-sectional views of their beads are shown in **Photo. 3(a)(b)**. Where in (a), the weld root is not deposited with the molten metal.

In Fig. 7, the beam power density is varied by changing the beam power keeping beam diameter minimum on the specimen surface. The defects always appeared in such cases and the number of the defects has nearly a constant value for all w_b. These weld roots have the sharp needle configuration as is illustrated in the figure and shown in **Photo. 4 (a) (b) (c)**, and their weld roots are not deposited with the molten metal.

In **Fig. 8**, the radius of curvature r_R in the weld root is shown versus $\tilde{p}_p$. Clearly when the internal defects

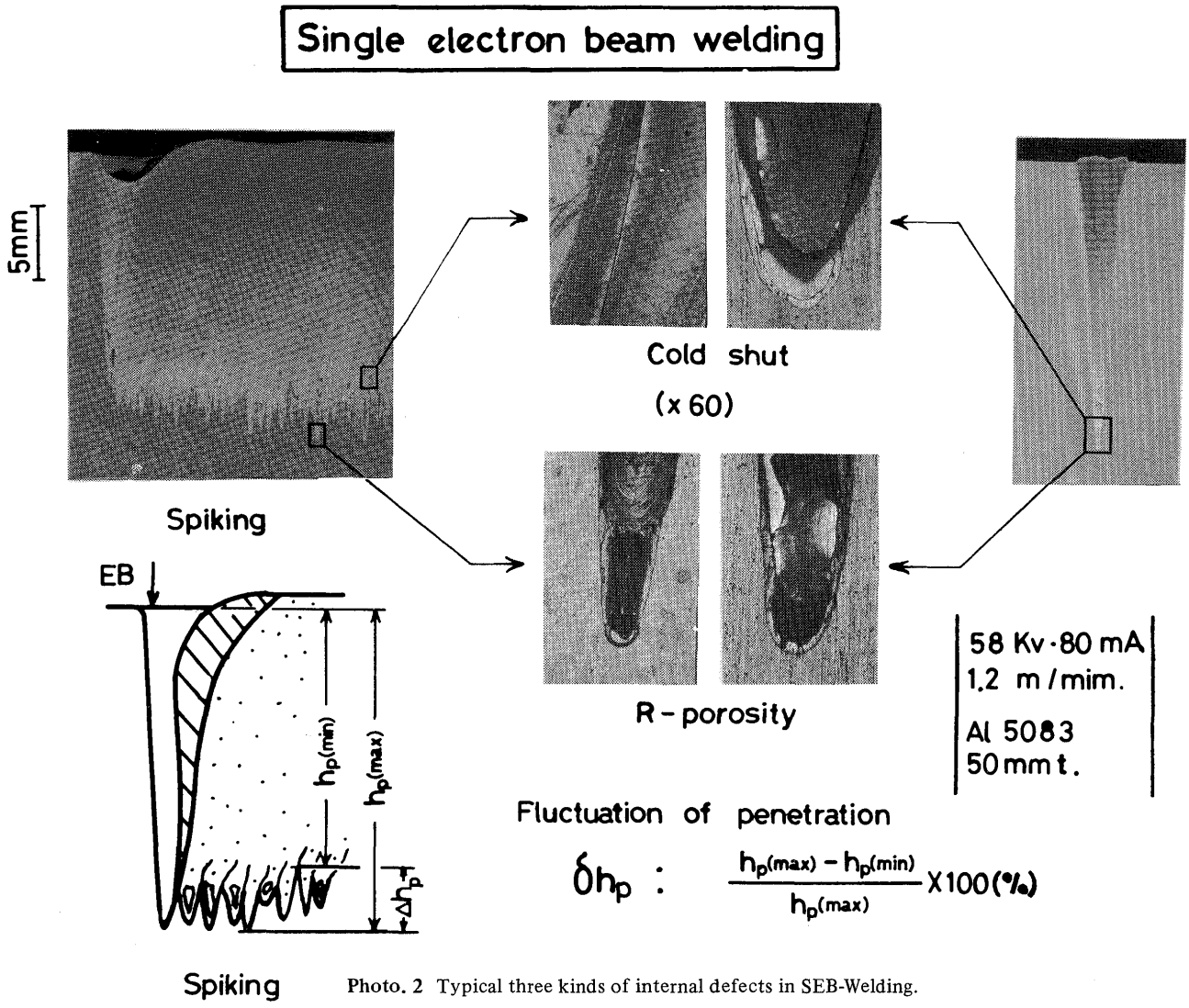

Photo. 2 Typical three kinds of internal defects in SEB-Welding.

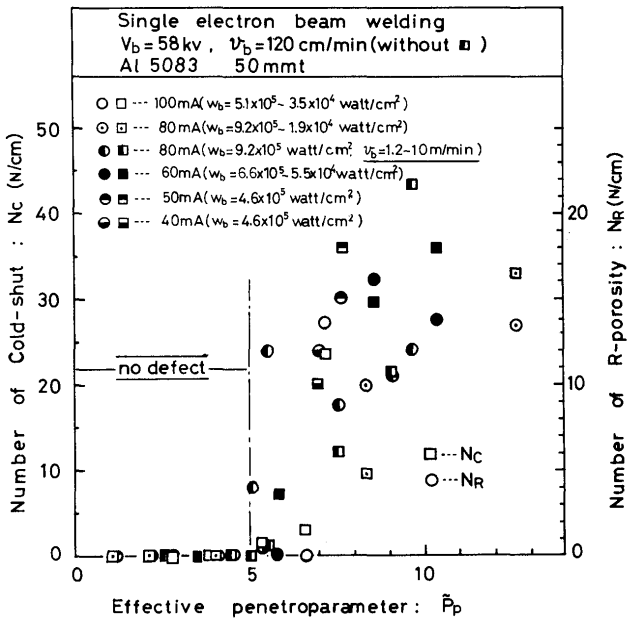

Fig. 5 Property of internal defects in various $\tilde{P}p$.

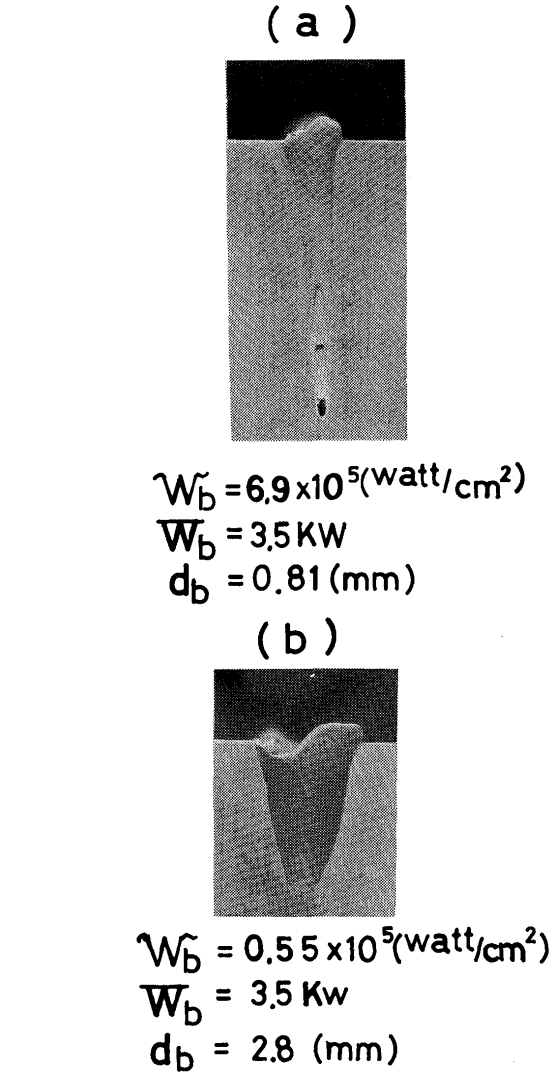

Photo. 3 (a) (b) Typical cross-sectional views of weld beads by wide and narrow diameter beans in Fig. 6.

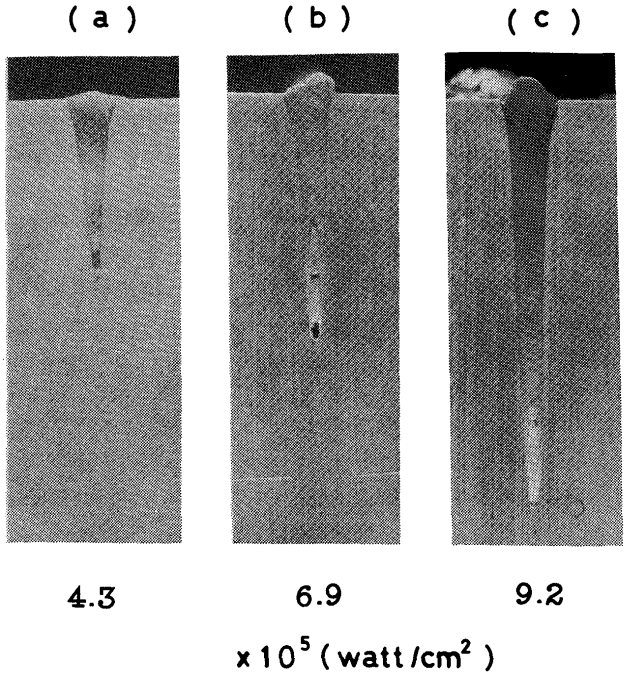

Photo. 4 (a) (b) (c) Sharp and needle weld root by narrow diameter beams in Fig. 7.

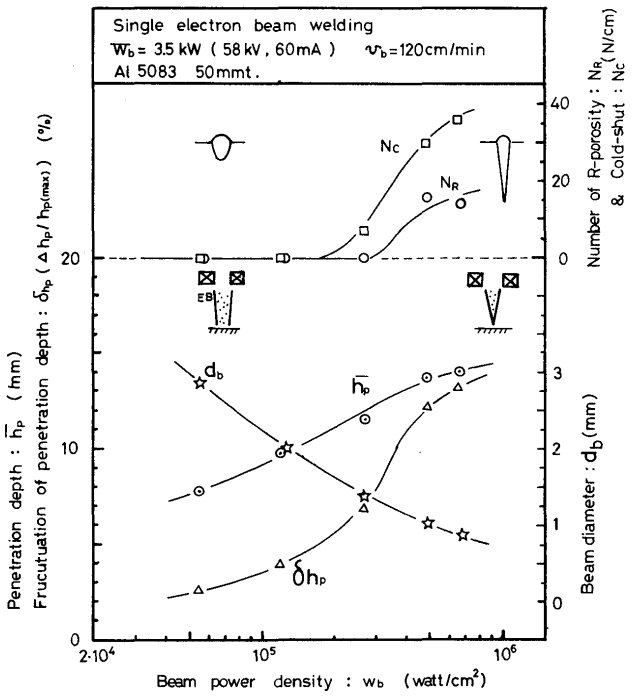

Fig. 6 Ocurrence of internal defects in various beam power densities by changing beam diam. at constant beam power.

appear, the radius of curvature in the weld root becomes a smaller value in larger $\tilde{p}_p$ as compared with the case of producing the no-defects beads which have a large radius of weld root in smaller $\tilde{p}_p$.

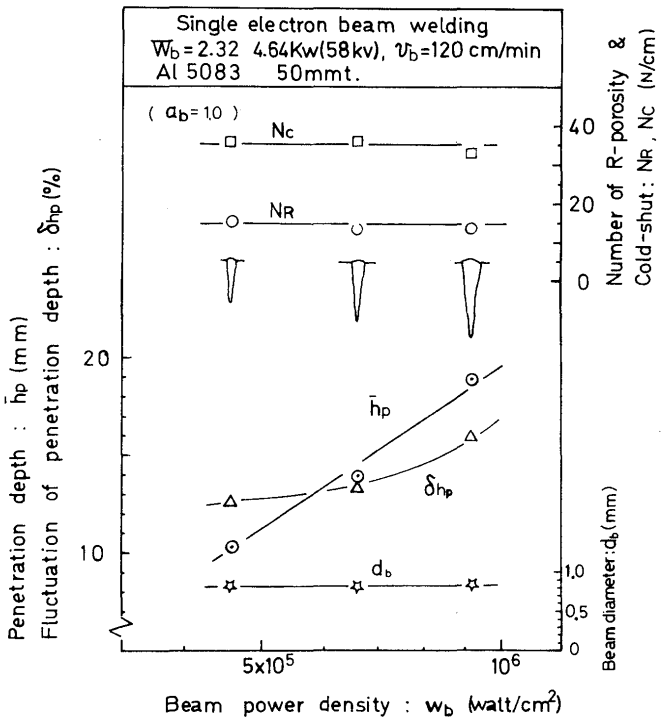

Fig. 7 Appearance of internal defects keeping minimum diameter of beam in various beam power densities.

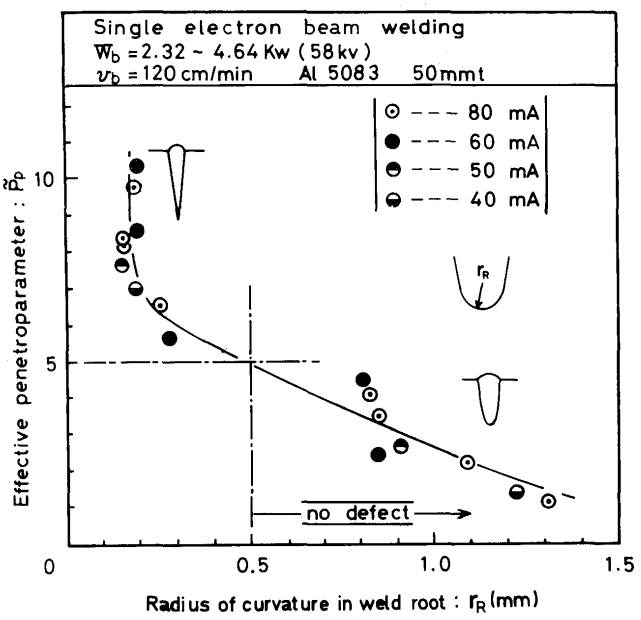

Fig. 8 Radius of curvature on weld root by SEB-Welding.

Cooling-rate by Single electron beam welding

r_R (mm)	d_b (mm)	Power density (watt/cm²)	N_R (N/cm)	N_C (N/cm)	Cooling-rate at 600°C (°C/sec)
0.20	0.98	6.1×10^5	9.5	10	1.2×10^4
0.88	2.95	6.8×10^4	0	0	1.5×10^3

58Kv 80mA 1.2m/min Al 5083

Table 2 Cooling-rate during Single electron beam welding.

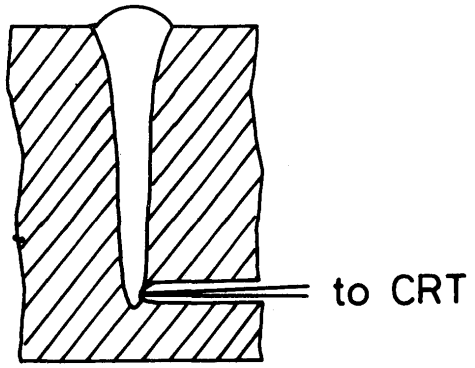

Fig. 9 Arrangement of thermo-cupple during welding.

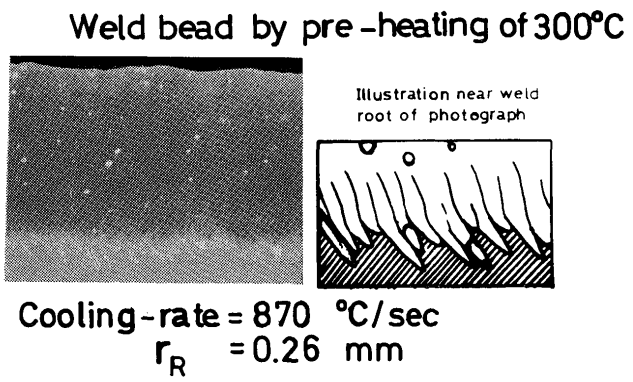

Photo. 5 Typical longitudinal section of weld bead in pre-heating of 300°C by SEB-Welding 58KV-80mA, 1.2 m/min, Al 5083.

We have also measured the cooling-rate of molten metal near the weld root during welding by the thermo-cupple which was arranged as is illustrated in **Fig. 9**. The results are summarized in **Table 2**. In case of the small raius of curvature in the weld root (r_R), the cooling-rate at 600°C (which is nearly equal to the melting point of the specimen used) is faster by 1-order than that of the large radius of weld root. On the other hand, for slowing down the cooling-rate in deep penetration, the specimen was pre-heated up to 300°C (which indicates almost the about half value of the melting point[7]). But it is not useful to prevent these defects as shown in **Photo. 5**, where the cooling-rate is very low enough (870°C/sec), but very small radius of curvature in weld root is formed and where is not deposited with molten metal. Moreover a new type defect of the large blowhole was caused by this pre-heating technique.

In the SEB-Welding, the occurrence of the internal defects is closely related with the configuration of weld root, and it is concluded that the sound bead formation with large radius of weld root would result in the shallow and wide bead of the smaller $\tilde{p}_p$.

Then we think, it is possible to prevent the internal defects by some proper means of depositting the weld root with the molten metal, for instance, widenning the radius of curvature on the weld root in deep penetration.

4. Tandem Electron Beam Welding

4.1 Principle of preventing internal defects

Fig. 10 shows the principle of preventing the internal defects by using the TANDEM ELECTRON BEAM. When we use only EB-1 of the high power density beam with small diameter, the internal defects of course appear in needle and deep penetration as shown in the photograph (a) of Fig. 10. While in the photograph (b) of Fig. 10, using only EB-2 in low power density of a wide diameter beam produces the large radius of curvature on the shallow and sound weld root. Now, when this EB-2 is impinged at the impinging point of the EB-1 as is illustrated in the schematic figure (c) of Fig. 10. EB-2 penetrates quite easily over the depth made by EB-1, and the new and wide weld root is created, in which the molten metal easily fill up and is deposited. As the result, the cooling-rate itself at the weld root becomes low. In this way, the internal defects can be suppressed and the

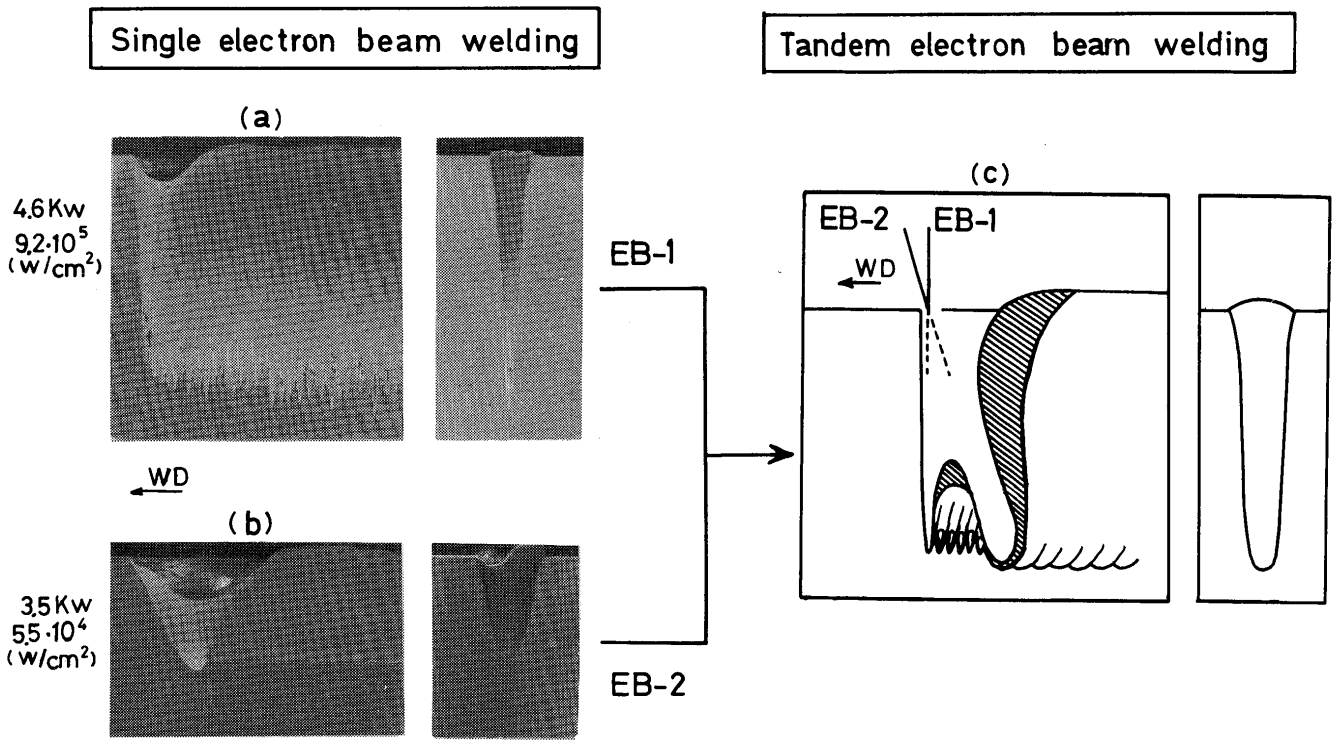

Fig. 10 Principle of preventing internal defects by TEB-Welding

sound bead is obtained with deep penetration by the TEB.

4.2 Optimum Penetration Mode of EB-2 for Preventing Internal Defects

In **Fig. 11**, the occurrence of internal defects is shown versus the power density of EB-2 by changing the beam diameter (d_b) at the constant power. The change of defects number corresponds well with the penetrating modes of EB-2, therefore the situation of the occurrence of defects can be classified into A, B, C three Regions. The crater-cavities of three Regions are shown in **Photo. 6.**

[A-Region]; In this region, because the penetration depth of EB-2 which has a much wide beam diameter is smaller than that of EB-1, so the defects are remained at the weld root.

[B-Region]; In this Region, sound bead can be obtained in deep penetration. EB-2 which is properly controlled beam diameter penetrates some bit over the depth of EB-1, so the weld root has a large radius of curvature and is deposited with the molten metal completely.

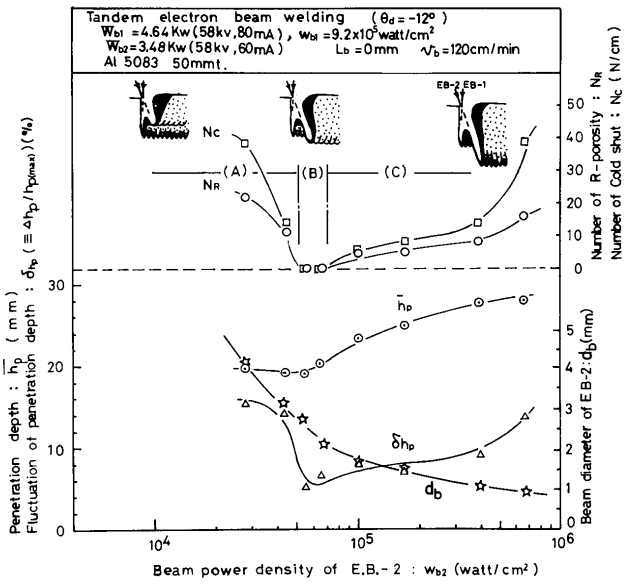

Fig. 11 Change of defects number and weld bead parameters by TEB.

To clarify the configuration and behavior of the beam hole in detail during welding, two kinds of the direct observation method were used as is schematically shown in **Fig. 12** and **13**.

One is named-for the "direct luminous observation method[8]" as shown in **Fig. 12**, the heat proof-glass was in contact with the side of a specimen and the TEB was impinged along the boundary between this glass and specimen. In this case the damege of glass is minor, therefore the behaviors of the beam hole in the metal specimen can be directly observed througth the glass. The profile of this beam hole is shown in **Photo. 7 (a)**, in which the needle weld root formed by EB-1 is remelted

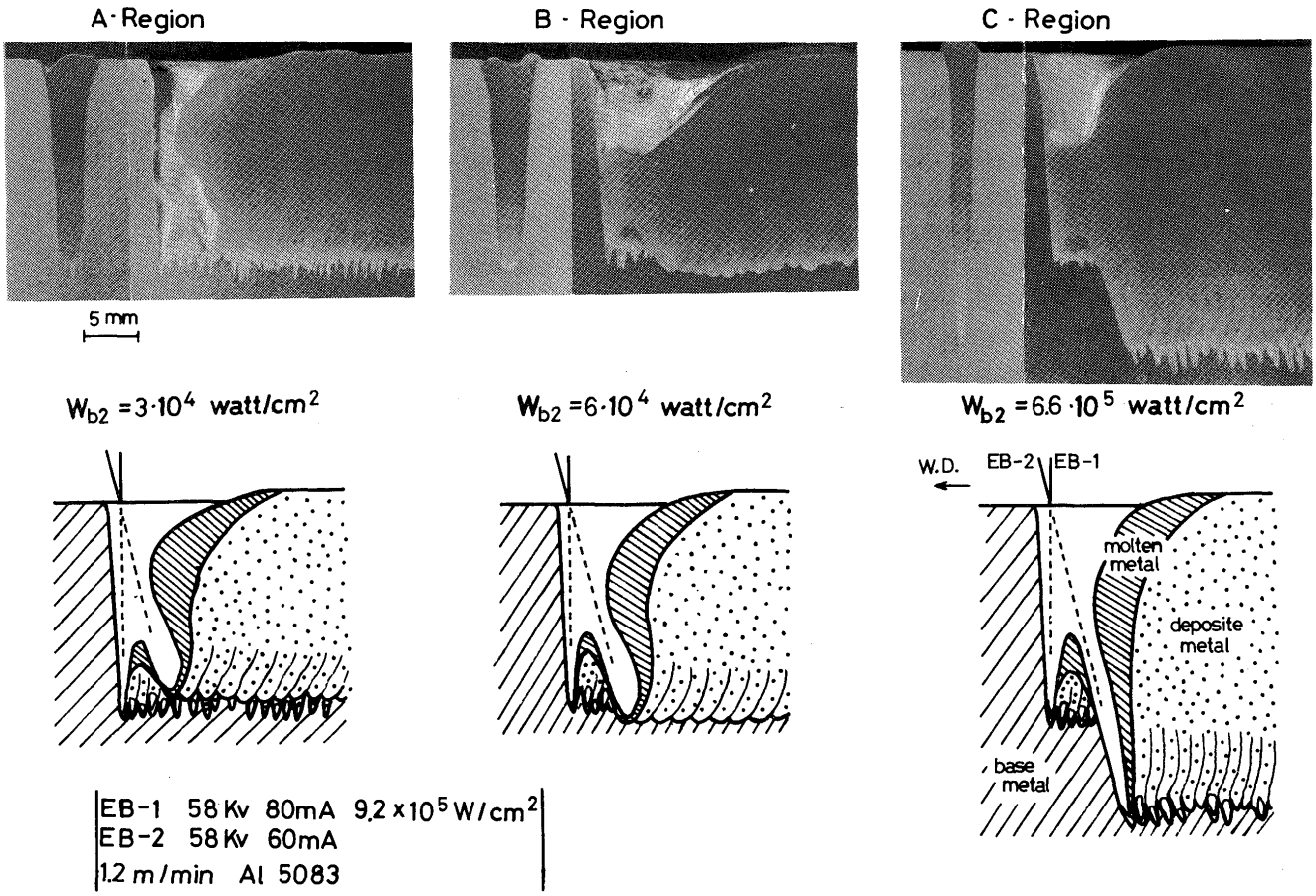

Photo. 6 Typical crater caties in A, B, C-Region by TEB-Welding

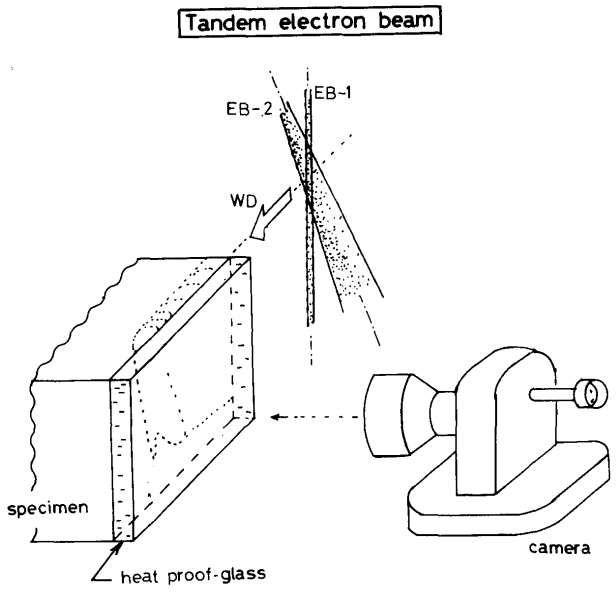

Fig. 12 Direct luminous observation method for beam hole behavior during welding.

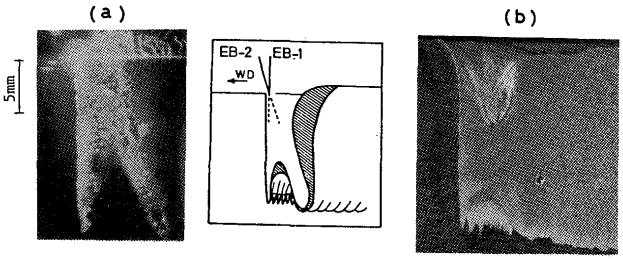

Photo. 7 (a) Appearance of Tandem beam hole by luminus observation method of Fig. 12 (800 fps).
(b) Longitudinal section by same welding parameters as (a).
58Kv 45mA (EB-1), 58KV 30mA (EB-2), 60 cm/min A1-7075 60 mmt.

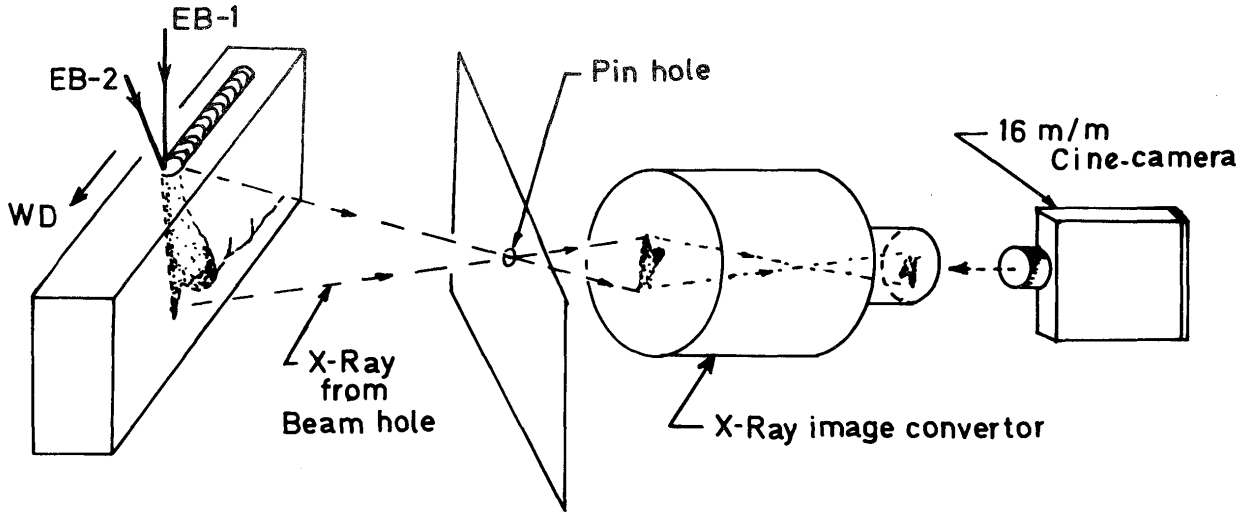

Fig. 13 Beam hole X-Ray observation method for beam hole behavior during welding.

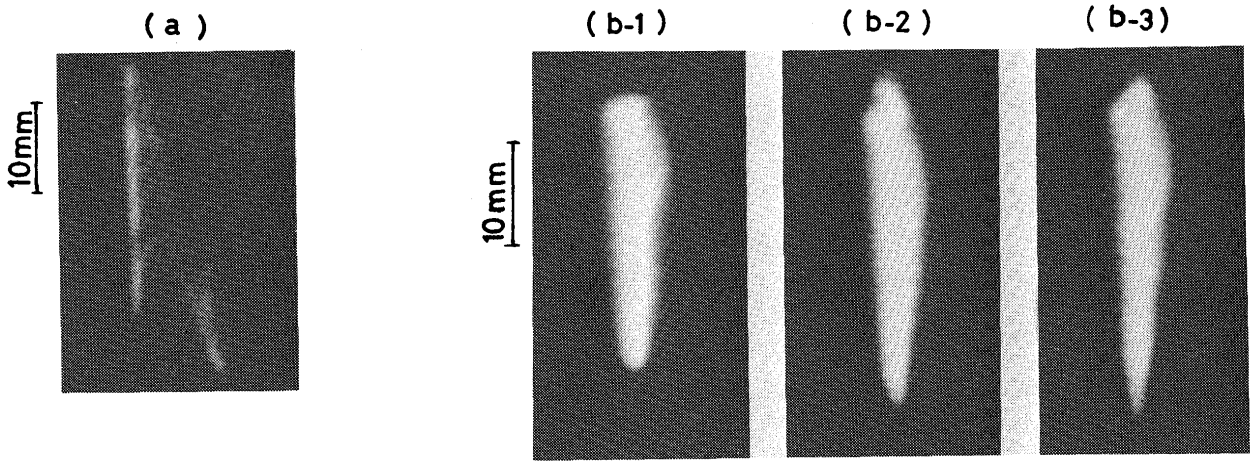

Photo. 8 Appearance of typical beam holes during welding by use of Beam hole X-Ray observation method as illustrated in Fig. 13, Al-7075, 60 mmt.
(a) Tandem-Beam hole, 58KV 60mA (EB-1) 58KV 45 mA (EB-2) 36cm/min, 150fps (1/375 sec).
(b) Single-Beam hole, 58KV-60mA, 1/30 sec. 45cm/min.

by a wide beam hole of EB-2. While, **Photo. 7 (b)** shows the weld bead produced by the conventional bead-on-plate welding using the same specimen and welding parameters. Both photographs correspond quite well each other in weld shape, spiking frequency and penetration depth.

Second is, in **Fig. 13**, named-for the "Beam hole X-Ray observation method", where the beam hole X-Ray is generated by the interaction between the welding electron beam and the materials of a specimen in the beam hole during welding. This X-Ray was focused on the input screen of X-Ray image-convertor through a pin-hole. Typical photographs are shown in **Photo. 8 (a)(b)**, where the shapes of beam hole are similar to the result of the direct luminus observation method and to the longitudinal cross-section of weld bead. It is useful to research the situation of the beam hole behavior by this Beam hole X-Ray technique, peculiar to the time and spatial dependent distrubutions of the perturbing interaction regions between the electron beam and inner walls in the beam hole during welding.

[C-Region]; EB-2 of a narrow diameter beam penetrates much over the depth of EB-1, they cause again the internal defects at the narrow weld root. In this case, the

spike like uneven-penetration is formed in the same process as is discussed in Chaper 3.

4.3 Characteristics of Weld Bead in B-Region

The dependence of the radius of weld root r_R on the effective penetroparameter $\tilde{p}_p$, the cooling-rate near the weld root are shown in **Fig. 14** and **Table 3** respectively.

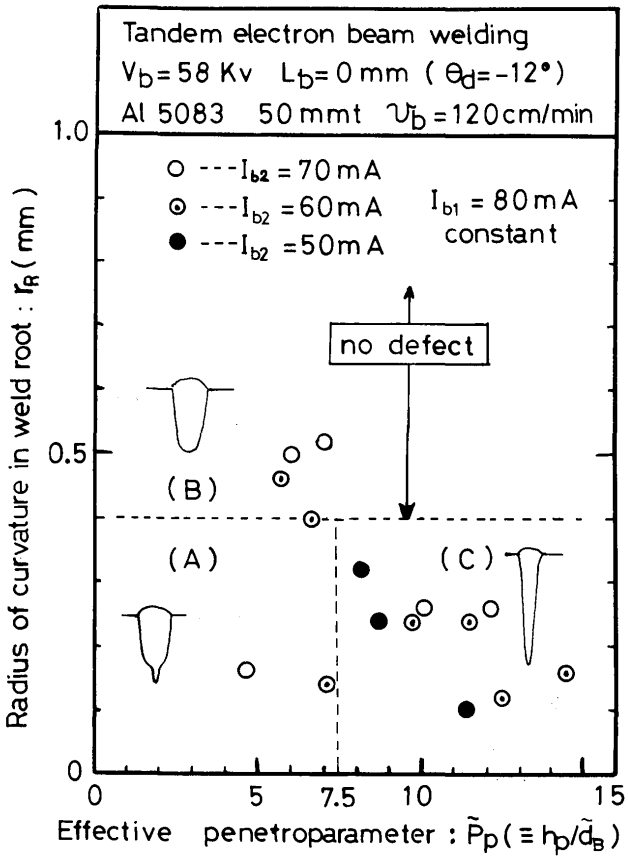

Fig. 14 Radius of curvature on weld root by TEB-Welding.

Methode	r_R (mm)	Power and Power densiy	Cooling-rate at 600°C (°C/sec)	N_R (N/cm)	N_c (N/cm)
Single	0.20	4.6KW, 6.8×10^5 w/cm^2	1.2×10^4	9.5	10
Tandem (in B-Region)	0.54	(EB-1) 4.6KW, 9.2×10^5 w/cm^2 (EB-2) 4.06KW, 4.5×10^4 w/cm^2	7.0×10^2	0	0

Table 3 Cooling-rates by SEB- and TEB-Welding.

In B-Region with no-internal defects of Fig. 14, the round shape of weld root having the large radius of curvature can be produced in the deep penetration condition of the high $\tilde{p}_p$ value. On the other hand, the cooling-rate in B-Region is reduced by 2-orders with large radius (r_R) in comparision with the case of the SEB-Welding. As was mentioned above, it is seen that the large radius of the weld root is completed with low cooling-rate and it brings about preventing the defects in deep penetration.

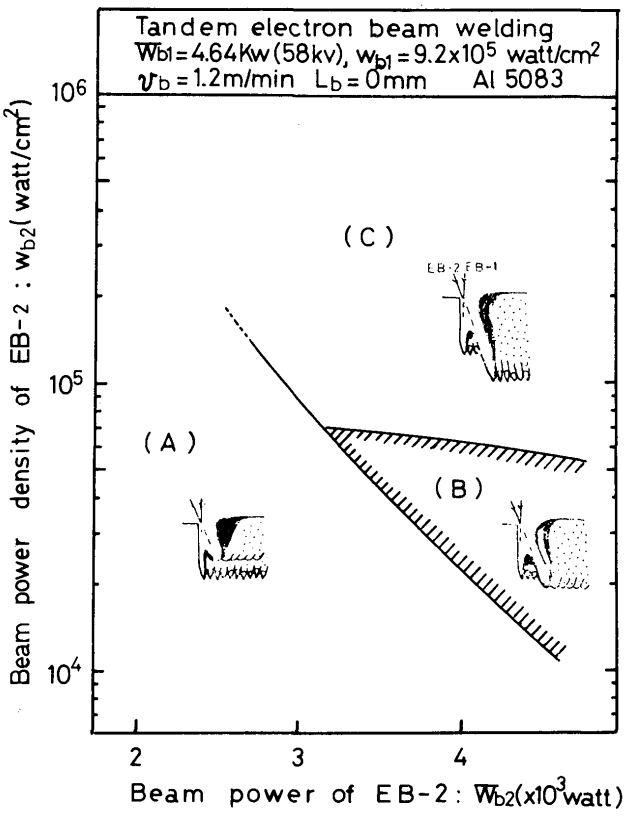

Fig. 15 Chart of preventing internal defects by expression of EB-2 power and density.

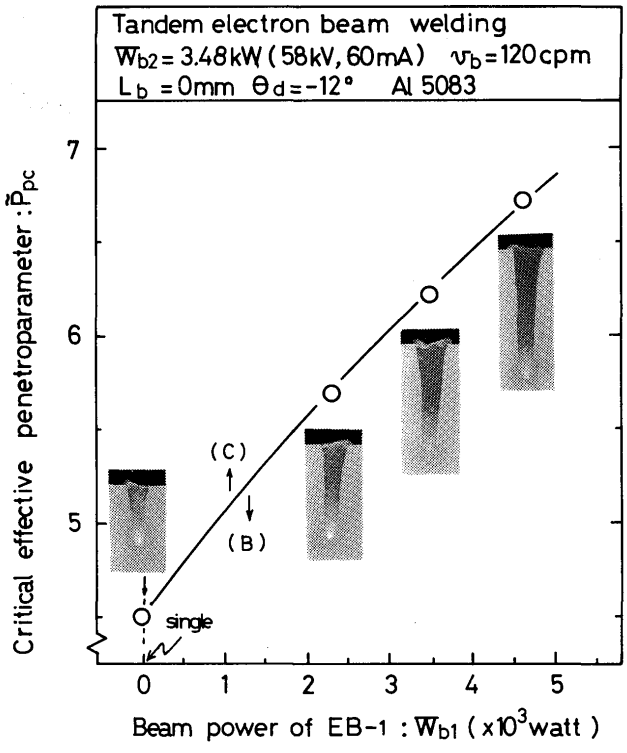

Fig. 16 Deep and sound bead formation by EB-1 power in TEB-Welding method.

4.4 Influluence of Beam Power

Fig. 15 shows the effects of beam power and power density of EB-2 on the typical penetrating modes of A, B, C three regions. By intensifying EB-2 power at the constant power of EB-1, B-Region can be enlarged quite easily in the TEB-Welding.

Next, the influence of EB-1 power on the critical value of the effective penetroparameter $\widetilde{p}_{pc}$ is shown in **Fig. 16**. The line $(\widetilde{p}_{pc})$ in the figure presents the transition from B to C-Region. For each plot, the power density of EB-2 is selected properly to prevent the internal defects under the constant beam power of EB-1.

A linear increase of this critical value $(\widetilde{p}_{pc})$ with the beam power of EB-1 indicates clearly that the deep and sound bead formation which can never be attained in the SEB-Welding, becomes possible at the very high power EB-Welding.

5. Conclusion

In this study, the fundamental parameters governing the formation phenomena of the internal defects such as Spiking, Cold-shut and R-Porosity are investigated in case of the conventional single electron beam welding, and the prevention of the internal defects are proved by the use of the TANDEM ELECTRON BEAM WELDING method. Their preventing process are discussed. Results obtained are stated as follows;

(1) In the deep penetration welding by the SEB-Welding method, the occurrence of the internal defects is closely related with the configuration of the weld root with small radius of curvature inherently formed by the high power density beam in small diameter. In this case, the molten metal is hardly deposited and its cooling-rate near the weld root is very fast in comparison with the case of shallow and wide sound weld bead produced by the use of a wide diameter beam with low power density.

(2) By the use of the TEB-Welding method, the occurrence of these internal defects can be sucessfuly prevented and sound bead is obtained even at the deep penetration condition. In this system, a wide diameter beam of EB-2 in low power density penetrates fully over the weld depth which contains the defects caused by a high power density beam of EB-1. And the large radius of curvature on the weld root is produced, and completely deposited with the molten metal in low cooling-rate.

Acknowledgement

We would like to thank Professor Dr. H. MARUO and Associate Professor Dr. S. MIYAKE for the kind and considerable discussion.

References

1) Y. Arata, K. Terai, F. Matsuda; "Study on Characteristics of Weld defect and its Prevention in Electron Beam Welding"; Report I, IIW, Doc. IV-112-73 (1973); Report II, IIW, Doc. IV-147-74 (1974); Report III, JWRI Vol. 3 No. 2 (1974), P81 ~88
2) L. N. Sayer; "Quality in Electron-beam Welding"; Brit. Weld. J., Vol. 14 No. 4, (1967) p163-9
3) F. Matsuda, T. Hashimoto, Y. Arata; "Some Metallurgical Investigation on Electron Beam Welding"; JWRI, Vol. 1, No. 1 (1973)
4) Y. Arata, E. Nabegata; "Tandem Electron Beam Welding"; IIW, Doc. IV-227-77 (1977); Report I, JWRI, Vol. 7, No.1 (1978) P101 ~109
5) Y. Arata; "Terms and Definitions for Electron Beam Welding, Laser Welding and Laser Cutting Used in Japan", IIW, Doc. IV-229-77 (1977)
6) R. A. Chihoski; "Understanding Weld Cracking in Aluminum Sheet"; Welding Journal, Vol. 51, No. 1 (1972) P9S ~ 18S
7) M. S. Tucker and A. Phillips "The influence of Cooling Rates on the microstructure and strength of 2014 Aluminum Alloy Welds"; Welding Journal, Vol. 47, No. 2 (1968) P82SS ~89S
8) Y. Arata, E. Abe, E. Nabegata and M. Fujisawa; "Dynamic Welding Phenomena during EB-Welding"; Part II, 2nd CISFFE (1978) p13-28.